SCIENTIFIC CULTURE
www.sci-cult.com

SCIENTIFIC CULTURE, Vol. 12, No. 5.1, (2026), pp. 1157-1164
Open Access. Online & Print

DOI: 10.5281/zenodo.12511091

STATIC STRUCTURAL ANALYSIS OF AN E-BUGGY CHASSIS USING FINITE ELEMENT METHOD

Natee Tanman[1], Nattaned Kongtabtim[2], Teerawat Klabklay[3*]

[1,2] Department of Power Engineering Technology, College of Industrial Technology, King Mongkut's University of Technology North Bangkok, Bangkok, Thailand
[3] Research Centre for Combustion Technology and Alternative Energy—CTAE, King Mongkut's University of Technology North Bangkok, Bangkok, Thailand

Received: 11/12/2024
Accepted: 25/02/2025

Corresponding author: Teerawat Klabklay
(teerawat.k@cit.kmutnb.ac.th)

ABSTRACT

This article aims to evaluate the stress and displacement distributions of an E-buggy chassis to verify its structural safety. Because the chassis acts as the primary structure that supports all vehicle loads and the suspension system, the body of the E-buggy was excluded from this analysis. The Finite Element Method (FEM)—an effective numerical approach for simulating solid mechanics—was utilized for the analysis. Furthermore, this study investigates the accuracy of FEM results using two meshing techniques: solid-element and beam-element meshing. The results indicate that the beam-element approach is comparable to the solid-element model, yielding an average error of less than 5 percent. Notably, beam-element meshing significantly reduces the number of elements, thereby accelerating computation time. Consequently, the beam-element approach was selected for the FEM analysis of the E-buggy chassis. Under static loading, the results showed a maximum stress of 39.48 MPa, a maximum displacement of 1.058 mm, and a minimum factor of safety of 5.95.

KEYWORDS: Finite Element Method, Static Structural Analysis, E-buggy Vehicle, Chassis

1. INTRODUCTION

An E-buggy is a compact electric vehicle used for versatile applications such as providing intra-campus shuttle services for a university [1]. Two major components of an E-buggy structure consist of the chassis and body, as illustrated in Fig. 1. Typically, in body-on-frame vehicles, the body is considered a non-load-bearing entity, supporting only its own mass [2,3]. Structural loads are predominantly absorbed by the chassis frame, which supports all vehicle loads and the suspension system. The Finite Element Method (FEM) is an effective tool for predicting structural strength in vehicles [4], allowing engineers to simulate stress distributions and deformation patterns under various loading conditions to verify its structural safety and durability standards prior to physical prototyping. The aim of this study is to evaluate the stress and displacement distributions of an E-buggy chassis using FEM to identify critical locations and ensure that the designs meet safety requirements through static load analysis. In addition, the FEM results from two meshing techniques: solid-element and beam-element meshes were investigated by comparing them with experimental data and analytical solutions of the two validation cases: tensile testing and bending and deflection of a beam. Consequently, the most appropriate approach was then selected for the FEM analysis of the E-buggy chassis.

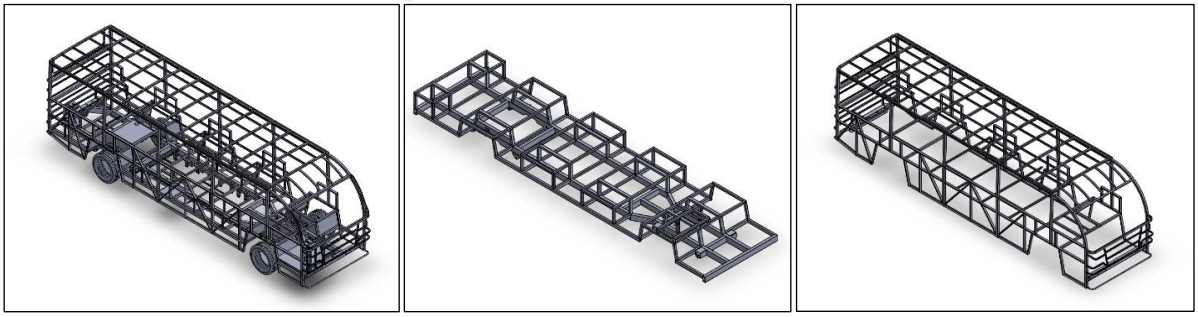

(a) (b) (c)

Figure.1: E-buggy structure: (a) Overall structure, (b) E-buggy chassis, (c) E-buggy body

2. THEORY

2.1. Finite Element Method

The Finite Element Method (FEM) is a numerical technique used to solve solid mechanics problems governed by Hooke's law by discretising a structure into small elements. The abbreviated finite element equation [5] is expressed in Eqs. (1).

$$[K]\{\delta\} = \{F\} \quad (1)$$

where, $[K]$ is the element stiffness matrix (N/m)

$\{\delta\}$ is a vector of nodal displacements (m)

$\{F\}$ is a vector of nodal forces (N)

Generally, the external force vector $\{F\}$ and element stiffness matrix $[K]$ are known, which are used to calculate the displacements $\{\delta\}$. Once the displacements are known, the strain can be determined using Eqs. (2).

$$\{\varepsilon\} = [B]\{\delta\} \quad (2)$$

where, $\{\varepsilon\}$ is a vector of nodal strain (m/m)

$[B]$ is a matrix of the derivation of the shape function $(1/m)$

The vector of nodal stress can be calculated from the vector of nodal strain $\{\varepsilon\}$ by Hooke's law expressed in Eqs. (3).

$$\{\sigma\} = [C]\{\varepsilon\} \quad (3)$$

where, $\{\sigma\}$ is a vector of nodal stress (Pa)

$[C]$ is the stiffness material matrix (Pa)

2.2. Bending and Deflection of Beam

According to the elastic flexure formula for pure bending, the maximum normal stress (σ_{max}) is given by Eqs. (4). For a simply supported beam under the loading shown in Fig. 2, the maximum deflection of the beam (y_{max}) can be determined using the elastic curve equation [6], as expressed in Eqs. (5).

$$\sigma_{max} = \frac{Mc}{I} \quad (4)$$

where, M is the bending moment in a beam $(N \cdot m)$

I is the moment of inertia (m^4)

c is the largest distance from the neutral surface (m)

$$y_{max} = -\frac{PL^3}{48EI} \quad (5)$$

where, P is a concentrated load acting on the beam (N)

L is the length of the beam (m)

E is the elastic modulus of the beam material (Pa)

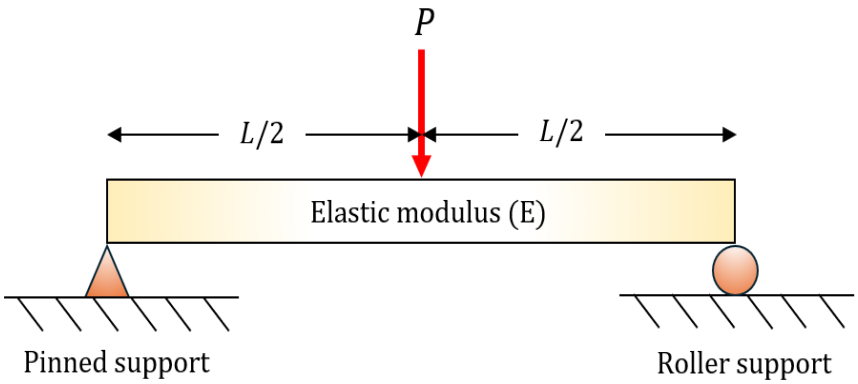

Figure 2: Simply supported beam with a concentrated load

2.3. Distortion Energy Theory

A well-known failure theory to predict behavior of ductile materials is the 'Distortion energy' or 'von Mises criterion'. The theory states that yielding occurs when the von Mises stress reaches the yield strength of the material under uniaxial tension [7,8] as shown in Eqs. (6).

$$\sigma_V = S_Y \quad (6)$$

where, σ_V is von Mises stress (Pa)
S_Y is yield strength (Pa)

$$\sigma_V = \sqrt{\frac{(\sigma_1 - \sigma_2)^2 + (\sigma_2 - \sigma_3)^2 + (\sigma_3 - \sigma_1)^2}{2}} \quad (7)$$

where, $\sigma_1, \sigma_2, \sigma_3$ are principal stresses (Pa)

To prevent object failure in static structural design, the factor of safety (F.S.) is applied, as defined in Eqs. (8).

$$F.S. = \frac{S_Y}{\sigma_V} \quad (8)$$

3. VALIDATION CASES

This section introduces two mesh generation techniques – solid-element and beam-element meshing – employed to solve 3D solid mechanics problems using the finite element method (FEM). Solid-element mesh is used in volumetric discretization, whereas beam-element mesh acts as a 1D element ideal for line-based or truss structures [5]. Its advantage is that it uses significantly fewer elements, allowing for faster calculations without compromising accuracy. This section attempts to verify that the beam-element meshing technique can be used appropriately in the FEM simulations. Two cases, specifically (i) tensile test and (ii) bending and deflection of a beam, are presented.

3.1. Tensile Test

The experimental tensile test data of the true stress-strain curve from Rafal M. Molak et al. (2009) [9] were used for comparison, as shown in Fig.3. The specimen geometry is illustrated in Fig. 4, which was made of 316L stainless steel. To investigate the differences in results, FEM simulations employing solid-element mesh and beam-element mesh techniques were conducted under the same boundary and loading conditions as shown in Fig. 5. One end of the specimen was fixed, while a tensile load was applied to the other. As illustrated in Fig. 3, the FEM results indicated that both meshing techniques provided nearly identical values of strain in both elastic and plastic regions. In addition, Fig. 6 demonstrates that, despite the large variation in mesh density, both solid-element mesh (3,040 elements) and beam-element mesh (120 elements) techniques predicted strains at tensile stress of 850 MPa that closely matched the experimental results. The average percentage errors of solid-element mesh and beam-element mesh FEM for strain values were 4.262% and 4.406%, respectively.

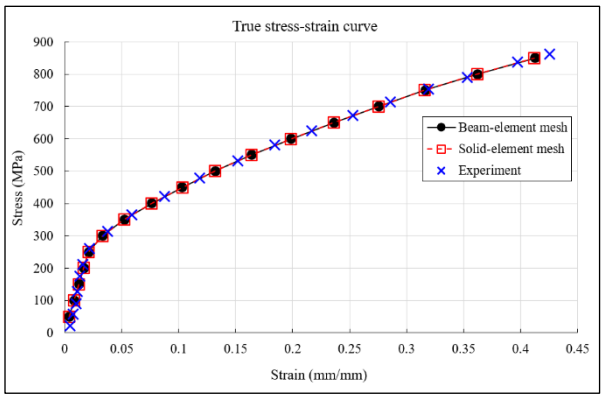

Figure 3: Comparison of experimental and FEM results: Solid-element and beam-element mesh

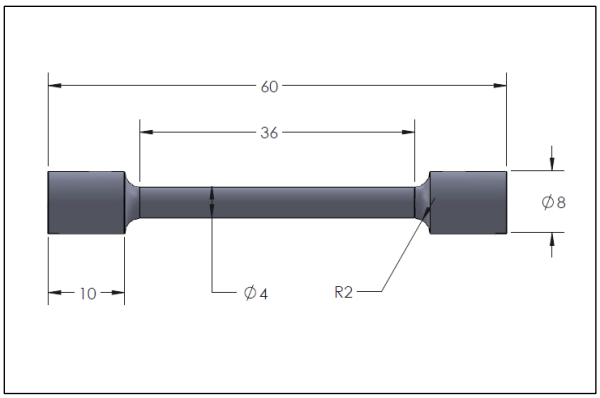

Figure 4: Specimen geometry for tensile testing (dimensions in mm) [8]

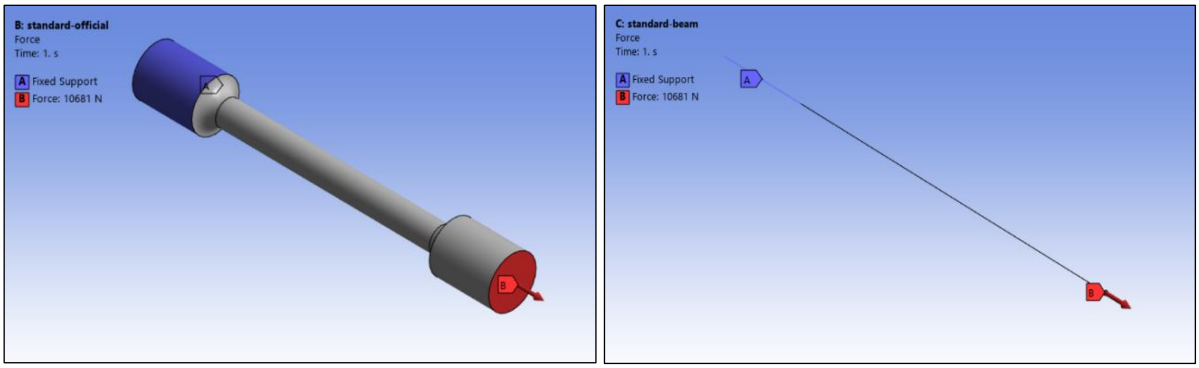

(a) (b)

Figure 5: Boundary and loading conditions setting: (a) Solid-element mesh, (b) Beam-element mesh

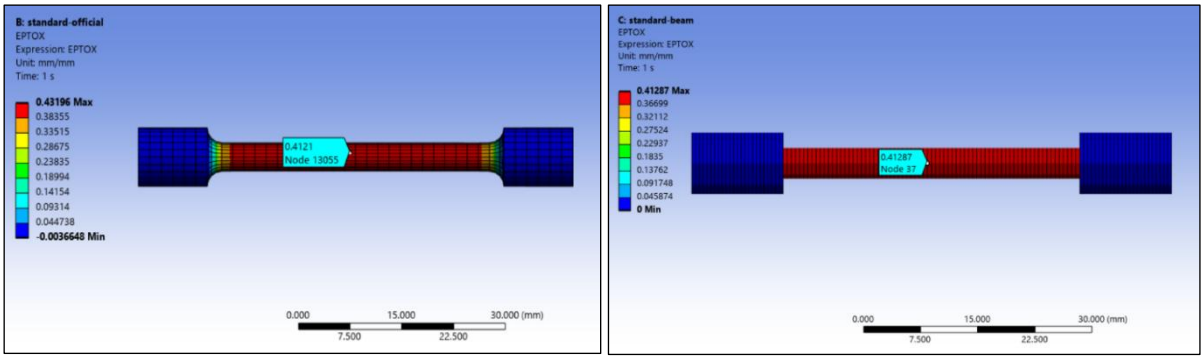

(a) (b)

Figure 6: FEM simulation results for tensile stress of 850 MPa: (a) Solid-element mesh, (b) Beam-element mesh

3.2. Bending and Deflection of a Beam

As illustrated in Fig. 7, a 100x100 mm square hollow-section ~~of~~ beam with a wall thickness of 5 mm was made of ~~a~~ structural steel [5]. This beam was simply supported by a pin and a roller, with a concentrated load applied at mid-span as shown in Fig. 8. The analytical solutions for maximum normal stress and deflection of the beam [6] were used to verify the FEM results from both meshing techniques. The boundary and loading conditions are presented in Fig. 8. As illustrated in Fig. 10, the FEM results showed that both mesh techniques provide nearly identical maximum normal stress and deflection values. Additionally, as shown in Fig.9, the FEM result demonstrated that despite the significant difference in mesh density, both solid-element mesh (60,800 elements) and beam-element mesh (80 elements) models yielded maximum normal stress and deflection values with a concentrated load of 12 kN that closely aligned with analytical solutions. For solid-element meshing, the average percentage errors for maximum normal stress and deflection of this beam were 1.987% and 0.044%, respectively. In comparison, the beam-element meshing yielded errors of 0.676% and 0.044%.

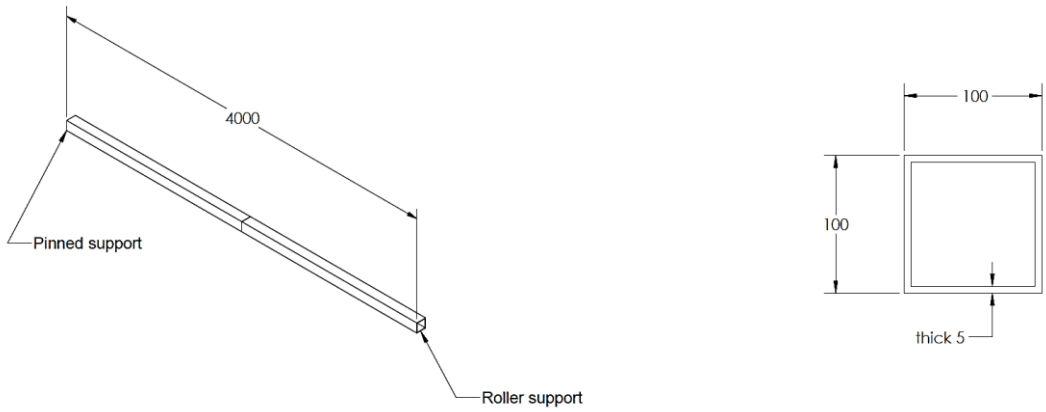

Figure 7: The simply supported beam with a square hollow-section (dimensions in mm)

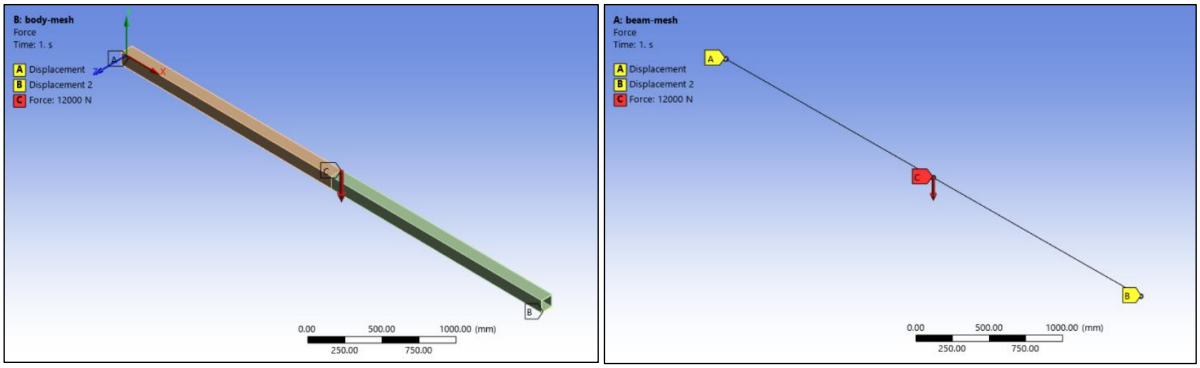

(a) (b)

Figure 8: Boundary and loading conditions setting: (a) Solid-element mesh, (b) Beam-element mesh

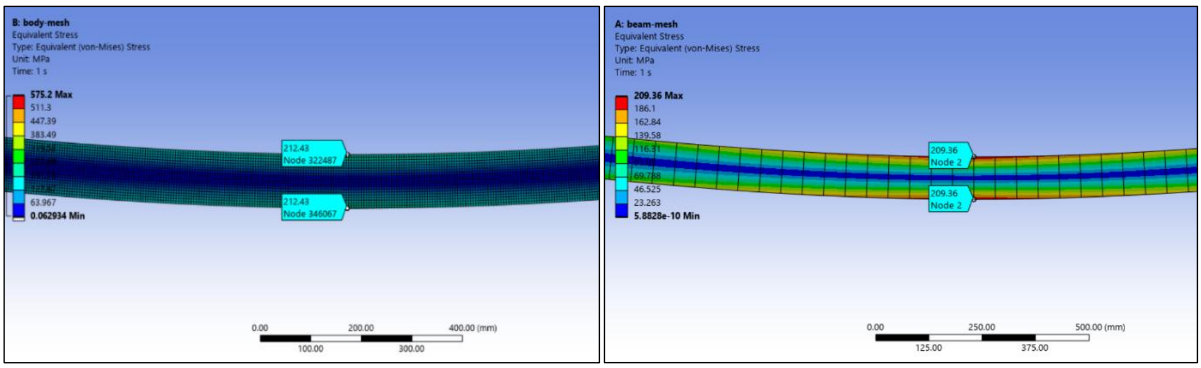

(a) (b)

Figure 9: FEM simulation results: (a) Solid-element mesh, (b) Beam-element mesh

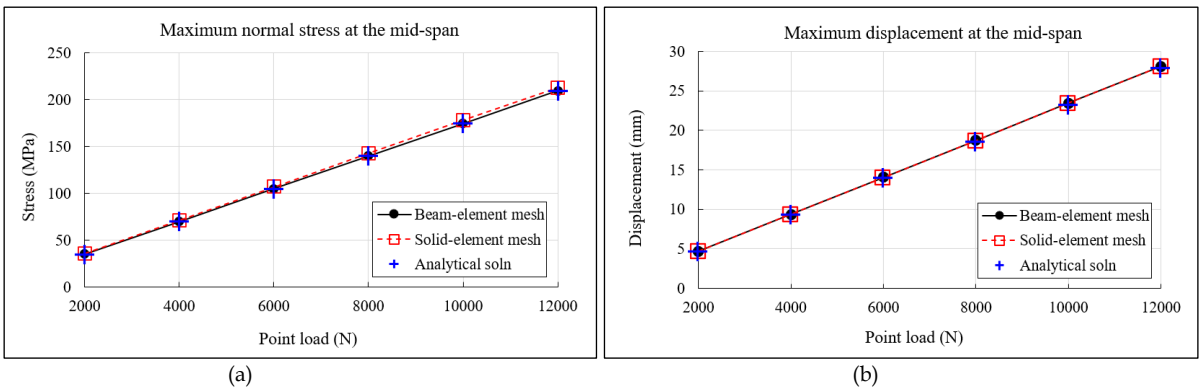

(a) (b)

Fig.10 Comparison of analytical solutions and FEM results at the mid-span beam: (a) Maximum normal stress, (b) Maximum displacement

4. RESULTS FOR THE E-BUGGY CHASSIS

Since the E-buggy chassis features truss geometry, employing beam-element meshing for the FEM analysis is more effective than using solid-element meshing, as discussed in Section III. The FEM analysis process consists of (A) 3D modeling, (B) mesh generation, (C) boundary and loading condition settings, and (D) calculation and analysis.

4.1. 3D Modeling

The structure of the E-buggy chassis, fabricated from structural members, had a width of 1.87 m and a length of 7.5 m. The chassis structure was designed and modeled using Ansys SpaceClaim software as presented in Fig. 11.

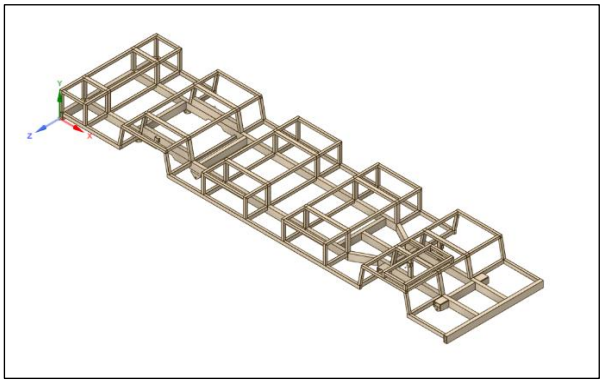

Figure 11: E-buggy chassis modeled in Ansys SpaceClaim software

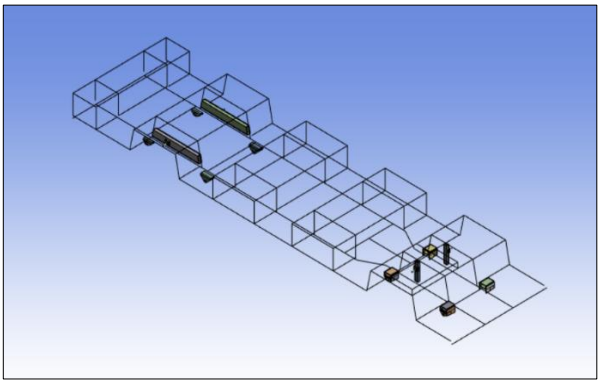

Figure 12: Beam line geometry of the E-buggy chassis

4.2. Mesh Generation

The 3D solid model of the E-buggy chassis structure was converted to beam-element geometry by extracting the structural member centerlines using Ansys SpaceClaim software, as illustrated in Fig. 12. Subsequently, these beam lines were discretized into a 1D beam-element mesh, as shown in Fig. 13.

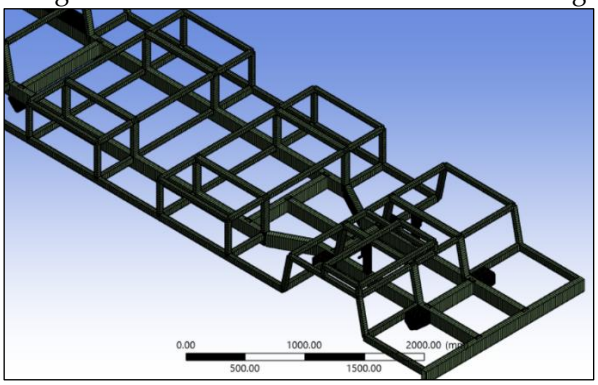

Figure 13: Beam-element mesh in E-buggy chassis

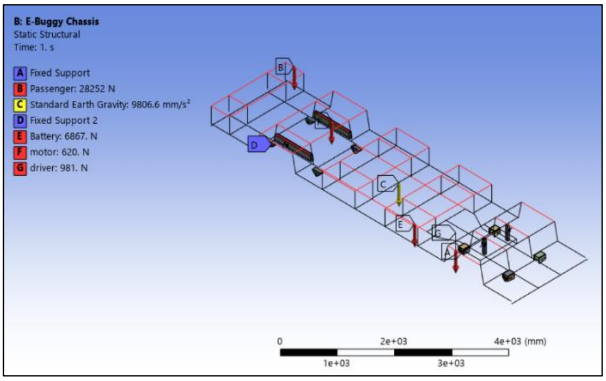

Figure 14: Boundary and loading condition setting

4.3. Boundary and Loading Condition Setting

The E-buggy chassis structure was made of Q235 steel [10], and its mechanical properties are listed in Table I. As shown in Fig. 12, eight fixed supports were applied at points A and D. The loading conditions included a passenger weight of 2,880 kg, a battery weight of 700 kg, a motor weight of 63 kg, and structural self-weight.

Table I: Material Properties [10]

Parameter	Q235	Unit
Density	7850	kg/m^3
Elastic modulus	200	GPa
Poisson's ratio	0.3	-
Yield strength	235	MPa

4.4. Calculation and Analysis

The boundary and loading conditions for the E-buggy chassis structure were applied and analyzed using Ansys Mechanical, as shown in Fig. 14. The von Mises stress and displacement distributions were investigated to examine critical points and the factor of safety of the chassis. As illustrated in Fig. 15, the maximum stress of 39.48 MPa was observed near the mid-span of the main beams of the chassis. Simultaneously, the maximum displacement reached 1.058 mm along the mid-section of the chassis sides.

These results were verified through a grid independence test to ensure that the mesh density was optimal, as illustrated in Fig. 16. Based on the distortion energy theory (von Mises yield criterion), the factor of safety is calculated as the ratio of the yield strength to the von Mises stress. Therefore, the minimum factor of safety for the E-buggy chassis was 5.95, indicating a high level of safety under the static structural loads for this article.

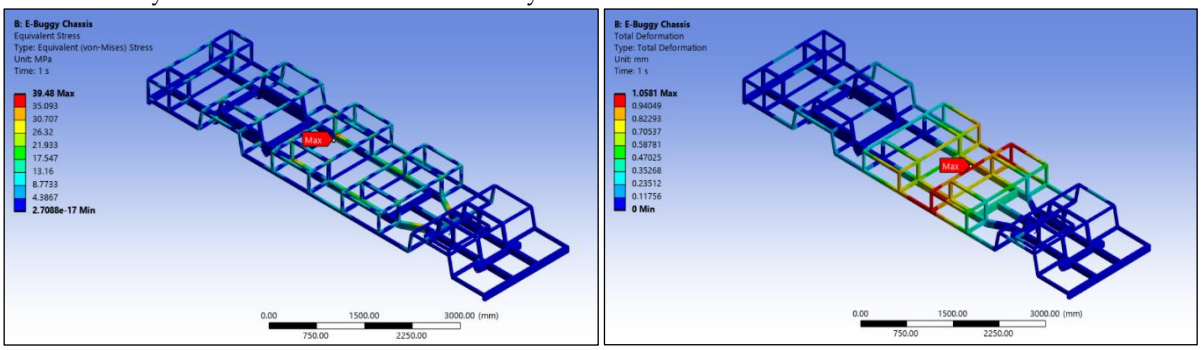

(a) (b)

Figure 15: FEM simulation results for E-buggy chassis: (a) von Mises stress, (b) Displacement

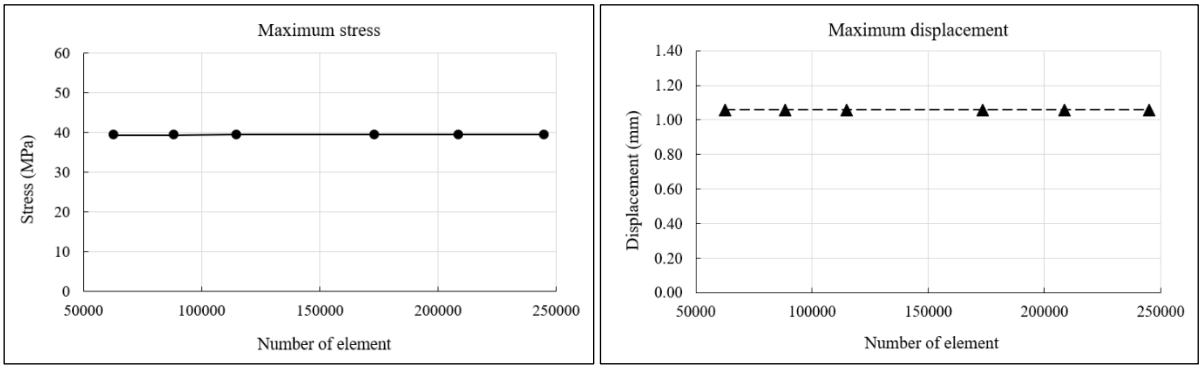

(a) (b)

Figure 16: Grid independence test results: (a) von Mises stress, (b) Displacement

5. CONCLUSIONS

This study evaluated the stress and displacement distributions of the E-buggy chassis using the Finite Element Method (FEM) to identify critical high-stress regions and ensure that the designs met safety requirements. The static structural analysis via FEM revealed a maximum stress of 39.48 MPa near the mid-span of the main beams, with a maximum deformation of 1.058 mm along the side sections. With a minimum factor of safety of 5.95, the chassis design demonstrates high structural strength under the applied static loading conditions.

ACKNOWLEDGEMENT

King Mongkut's University of Technology North Bangkok

REFERENCES

[1] Maini Materials Movement Pvt. Ltd., Bangalore, India, Value delivered. Always, 2016.
[2] C. Li, W. Qiu, W. Li, et. al., "Design and Experimental Validation of a Quarter-Car Pseudo-Active Suspension for Body-on-Frame Vehicles", Actuators, 15, 142, March 2026.
[3] K.R. Srinivasa, "Vehicle Body Engineering: Design, Materials, and Structural Analysis", World Journal of Advanced Research and Reviews, eISSN: 2581-9615, January 2020.
[4] T. Klabklay, Ch. Sumpavakup, A. Khumkrong, et. al., "Finite Element Analysis for Estimating Strength and Fatigue of the APM Structure", E3S Web of Conferences 602, 01012, January 2025.
[5] Ansys tutorials, Inc. 2020.
[6] F.P. Beer, E.R. Johnston, J.T. DeWolf, D.F. Mazurek, and S. Sanghi, "Mechanics of Materials 8 Edition in SI unit", McGraw-Hill Education, 2020.
[7] R. G. Budynas and J. Keith Nisbett, "Shigley's Mechanical Engineering Design 10 Edition", McGraw-Hill Education, 2015.
[8] D.R. Moss and M. Basic, "Pressure Vessel Design Manual 4 Edition", Elsevier Butterworth-Heinemann, December 2012.
[9] R. M. Molak, K. Paradowski, T. Brynk, et. al., "Measurement of mechanical properties in a 316L stainless steel welded joint", International Journal of Pressure Vessels and Piping, Vol. 86, 43–47, January 2009.

[10] European Assessment Document – EAD 200017-00-0302, "Hot rolled products and structural components made of steel grades Q235B, Q235D, Q345B and Q345D", European Organisation for Technical Assessment, 2016.